Electrochemical and Solid-State Letters, **15** (4) H91-H93 (2012)
1099-0062/2012/15(4)/H91/3/$28.00 © The Electrochemical Society

Ultraviolet Photo-Annealing Process for Low Temperature Processed Sol-Gel Zinc Tin Oxide Thin Film Transistors

Young Hwan Hwang, Seok-Jun Seo, Jun-Hyuck Jeon, and Byeong-Soo Bae[z]

Laboratory of Optical Materials and Coating, Department of Materials Science and Engineering, Korea Advanced Institute of Science and Technology (KAIST), Daejeon 305-701, Korea

Sol-gel zinc tin oxide (ZTO) thin film transistors (TFTs) were fabricated at a low temperature of 250°C using an ultraviolet (UV) photo-annealing process. A stable ZTO sol-gel solution was produced and showed considerable absorption in UV due to the incorporation of a chelating agent, acetylacetone, which also acts as a UV-activator. The UV photo-annealing and vacuum annealing improve the electrical performance of the ZTO TFT with mobility of 2 $cm^2/V \cdot s$ by effective dissociation of organic groups and promotion of metal-oxide-metal bonds formation, confirmed by X-ray photoelectron spectroscopy of the ZTO films.
 [DOI: 10.1149/2.013204esl]

Manuscript submitted October 19, 2011; revised manuscript received December 20, 2011. Published January 31, 2012.

Metal oxide semiconductors have attracted considerable interest as the active layer for thin film transistors (TFTs) in large area displays due to their high electron mobility, good uniformity, and high transparency.[1] Zinc oxide (ZnO), indium gallium zinc oxide (IGZO), zinc tin oxide (ZTO), and gallium zinc tin oxide (GSZO) are representative metal oxide semiconductors.[2–5] In particular, many studies on oxide semiconductor films deposited by a vacuum process have demonstrated high electrical performance with excellent environmental stability compared to conventional hydrogenated amorphous silicon (a-Si:H).[6,7] Several researchers have also reported solution-processed oxide TFTs. While the solution process affords simplicity, low cost, and high throughput, it requires high annealing temperature above 500°C to remove impurities and to promote metal-oxide-metal (M-O-M) condensation for realizing high performance oxide TFTs.[8,9] In efforts to overcome the limitation of the processing temperature of solution-processed oxide TFTs, oxide films have been prepared by various approaches such as chemical bath deposition (CBD), post-annealing, composition control, and the use low-temperature decomposable precursors.[10–13] Although these approaches can lower processing temperatures to 150–300°C, poor device performance and complex synthesis/fabrication process remain as problems of solution-processed TFTs.

Among various attempts to achieve low temperature fabrication, ultraviolet (UV) photo-annealing is a promising technique for sol-gel oxide films due to effective elimination of organic components and acceleration of M-O-M condensation by a combination of thermal annealing and UV irradiation.[14–16] In particular, photosensitivity endowed by the incorporation of UV absorbing compounds such as β-diketones in sol-gel solutions results in easy dissociation of organic species through UV photo-annealing.[15,17,18] However, low temperature preparation using UV photo-annealing has only been reported for some single oxide and ferroelectric multioxide films.

In this article, we report on the fabrication of sol-gel ZTO TFTs by UV photo-annealing at a low temperature of 250°C. Compared with thermal-annealed TFTs, the UV photo-annealed TFT exhibits enhanced transistor performance and the consecutive vacuum annealing process yields mobility exceeding 2 $cm^2/V \cdot s$. In order to shed light on the mechanism underlying the enhanced performance obtained with UV photo-annealing, X-ray photoelectron spectroscopy (XPS) studies of the ZTO thin films were conducted.

The sol-gel solution employed in the fabrication of the ZTO thin films was prepared by dissolving zinc acetate ($Zn(CH_3COO)_2$, Aldrich) and tin chloride ($SnCl_2$, Aldrich) in 2-methoxyethanol. In order to stabilize the solution, the precursors were chelated with acetylacetone ($CH_3COCH_2COCH_3$, Aldrich). The details of the synthesis process can be found in a previous report.[19] Bottom gate/top contact structured TFTs were fabricated by deposition of the resulting solutions on heavily boron (p+) doped silicon wafers covered with a thermally grown SiO_2 (100 nm) layer via spin-coating. The Figure 1a shows the structure of ZTO TFT. The deposited films were then annealed at 250°C for 1 h on a hot plate with UV (220–260 nm) light irradiation using a 1000 W Hg/Xe lamp optical system (82511, Oriel, Stratford, CT) under ambient atmosphere. Inset of Figure 1b shows the scheme of the UV photo-annealing process. After the UV photo-annealing step, the samples were annealed under vacuum ($<10^{-1}$ torr) at 250°C for 2 h with raise rate of 100°C/min using a rapid thermal annealing (RTA) system. Aluminum source and drain electrodes of 100 nm thickness were deposited by E-beam evaporation on the ZTO films. The channel length and width of the ZTO TFTs were 100 μm and 1000 μm, respectively.

UV absorption of the precursor solution was measured using a UV-visible-near infrared spectrophotometer (Shimadzu UV3101PC). The transfer characteristics of the ZTO TFTs were measured with a HP 4155A semiconductor parameter analyzer at room temperature in a dark box. XPS was employed to evaluate the change of chemical structures of the ZTO films during the UV photo-annealing and vacuum annealing steps.

Figure 1b shows the UV absorption spectra of the precursor solution. The maximum absorption of the solution was observed at around 280 nm and is attributed to the chelated acetylacetone groups.[20] From this analysis, it is expected that the solution is not only highly stable against precipitation but is also susceptible to activation under UV irradiation, which results in reduced fabrication temperature via UV photo-annealing.

Figure 2 shows the change of the transfer characteristics of the drain current (I_D) versus gate voltage (V_G) behavior at a drain-to-source voltage (V_{DS}) of 40 V for the sol-gel ZTO TFTs fabricated via the UV photo-annealing process. The TFT with only thermal-annealed ZTO thin film is not activated; do not exhibit any n-channel transfer characteristics, due to the insufficient thermal energy for decomposition and oxide formation. The TFT annealed for 6 h shows negligibly improved performance in spite of longer time for decomposition of the precursor and M-O-M condensation. The TFT exhibits very low mobility of 0.3 $cm^2/V \cdot s$, a threshold voltage (V_{th}) of 26 V, a sub-threshold slope of 1.61 V/decade, and an on-to-off current ratio of 9.4×10^4, $V_{DS} = 40$ V. By contrast, the UV photo-annealing process noticeably enhances the on-current of the ZTO TFT and contributes to plain on-off characteristics of transistors. This result is not attributed to the simple thermal effect of UV light; instead it is ascribed to electron excitation in the film induced by the UV photo-annealing. The $\pi \rightarrow \pi^*$ transition of UV absorbing species in the film gives rise to the dissociation of organic groups and the promotion of M-O-M bonds.[21] In addition, ozone and active oxygen species produced in the oxygen atmosphere under UV irradiation can oxidize suboxides or hydroxyl (OH) groups and also accelerate the combustion of organic compounds.[22] After consecutive vacuum post-annealing, the on-current drastically increases and the turn-on voltage (V_{on}) is

[z] E-mail: bsbae@kaist.ac.kr

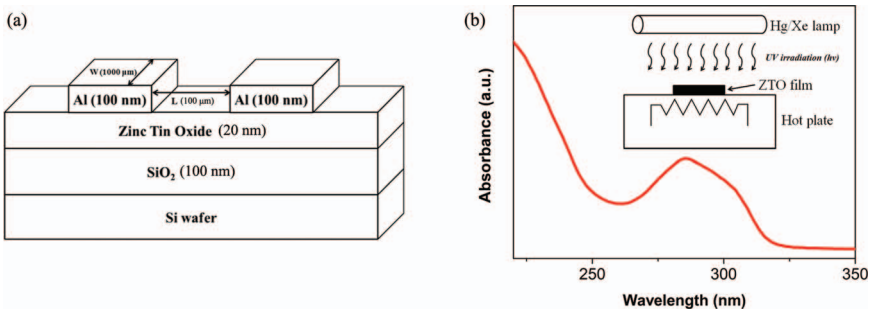

Figure 1. (a) Structure of ZTO TFT, (b) UV absorption spectra of the ZTO sol-gel solution, and (inset) scheme of UV photo-annealing process.

negatively shifted with a saturation mobility of 2 $cm^2/V \cdot s$, a threshold voltage (V_{th}) of 9 V, a sub-threshold slope of 1.35 V/decade, and an on-to-off current ratio of 1.7×10^6, $V_{DS} = 40$ V. The TFT performance in terms of mobility, on-to-off current ratio, and sub-threshold slope is improved substantially by adopting UV photo-annealing. This indicates that UV photo-annealing technique positively affects both formation of oxide and improvement of interface between semiconductor and gate dielectric in terms of traps. As documented in our previous report, the vacuum post-annealing process can generate oxygen vacancies, each of which donates two electrons to the conduction band, and eliminate residual Cl ions in the ZTO film.[11] Thus, higher carrier concentration results in improved characteristics with higher on current and saturation mobility of the ZTO TFT.

In order to investigate the effect of the UV photo-annealing process on the chemical and structural changes, the ZTO films were analyzed using XPS. Figure 3 shows the change of the O 1s and Cl 2p spectra of the ZTO films resulting from UV photo-annealing and vacuum post-annealing. The O 1s peaks (Figs. 3a–3d) are fitted by three nearly Gaussian binding energy curves centered at 530.2 eV, 531.4 eV, and 532.4 eV. The peak of the O 1s spectra with low binding energy at 530.2 eV (O_{OX}) is associated with the oxygen ions in the fully oxidized surroundings.[23] The medium binding energy peak at 531.4 eV (O_V) corresponds to the oxygen ions in oxygen deficient regions. The high energy peak at 532.4 eV (O_{OH}) is attributed to OH groups integrated into the materials and/or loosely bound oxygen on the surface from H_2O related species. The thermal-annealed films with 1 h and 6 h annealing time show similar area ratios of $O_{OH}/(O_{OX}+O_V+O_{OH})$, indicating the proportion of metal hydroxide (M-OH) species. This implies that M-OH species are not effectively converted to metal oxides due to the low thermal energy of the processing temperature. Compared with the thermal-annealed ZTO films, the UV photo-annealed film exhibits a smaller area ratio of $O_{OH}/(O_{OX}+O_V+O_{OH})$, which indicates that M-OH species are substantially reduced by the UV photo-annealing process. Under UV irradiation, reactive species are generated from the rupture of organic groups and the transition to an excited state by photon absorption, and consequently they effectively promote the formation of M-O-M bonds.[15] Thus, we can conclude that the activation energy for the M-O-M condensation is reduced by simultaneous UV irradiation and thermal-annealing. Meanwhile, after the consecutive vacuum post-annealing process, the area ratio of $O_V/(O_{OX}+O_V)$ increased from 0.22 to 0.39, which indicates that oxygen vacancies in the ZTO film increase in number during the vacuum annealing. The reduction of the concentration of Cl ions after vacuum post-annealing is also observed in the Cl 2p spectra (Figure 3e). These results imply that the prominent increase of the on current and saturation mobility by vacuum post-annealing originates from high carrier concentration generated by a large amount of oxygen vacancies as well as by the removal of the residual Cl ions, which act as defect sites.[11]

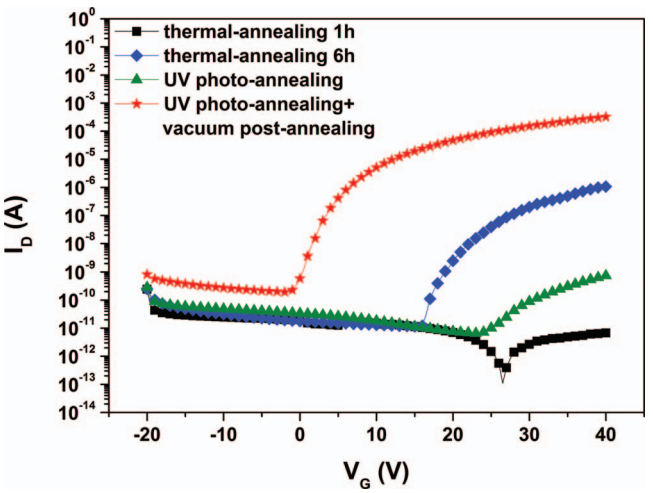

Figure 2. Transfer characteristics at $V_{DS} = 40$ V for the ZTO TFTs fabricated at 250°C by thermal-annealing (1 h and 6 h), UV photo-annealing, and UV photo-annealing followed by vacuum post-annealing.

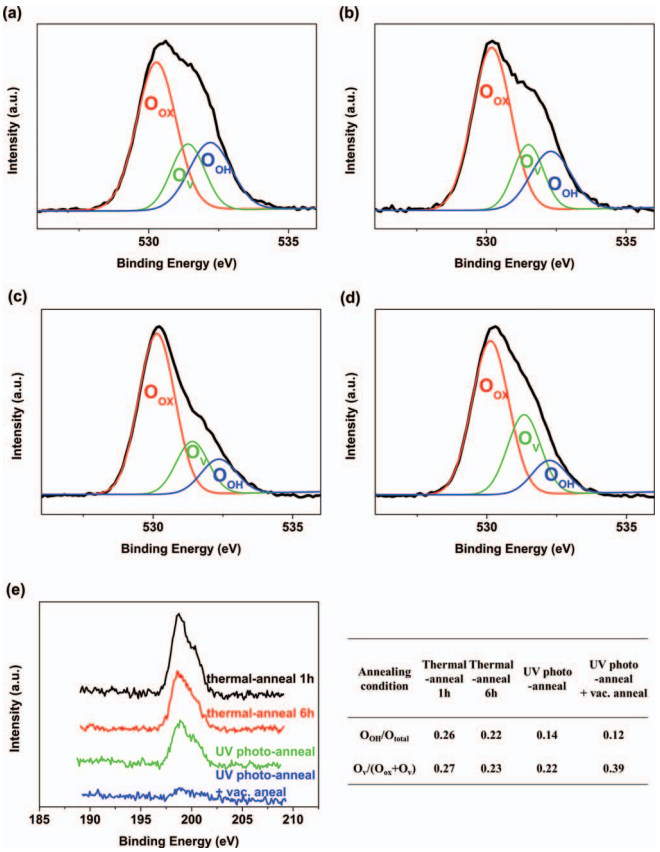

Annealing condition	Thermal -anneal 1h	Thermal -anneal 6h	UV photo -anneal	UV photo -anneal + vac. anneal
O_{OH}/O_{total}	0.26	0.22	0.14	0.12
$O_V/(O_{ox}+O_v)$	0.27	0.23	0.22	0.39

Figure 3. XPS spectra of O 1s of the ZTO films with (a) thermal-annealing for 1h, (b) thermal-annealing for 6h, (c) UV photo-annealing, and (d) UV photo-annealing followed by vacuum post-annealing, and (e) Cl 2p thereof.

In conclusion, we applied a UV photo-annealing process to achieve low temperature fabrication of sol-gel ZTO TFTs. The use of acetylacetone as a chelating agent for solution stability gives rise to effective photo-absorbality under UV light. Compared with the thermal-annealing process at 250°C, the UV photo-annealing enhances the electrical properties of the ZTO TFTs due to acceleration of the formation of M-O-M bonds. The subsequent vacuum post-annealing process further improves the performance, with mobility of 2 $cm^2/V \cdot s$ and an on-off current ratio of 1.7×10^6 being observed. These improvements are attributed to the generation of oxygen vacancies and the removal of Cl ions. The obtained results indicate that the UV photo-annealing is an effective process for low temperature preparation of sol-gel oxide semiconductors, and it can also be applied to the fabrication of devices on various substrate materials.

Acknowledgments

This research is financially supported by the Ministry of Knowledge Economy (MKE) and Korea Institute for Advancement in Technology (KIAT) through the Workforce Development Program in Strategic Technology. This work was supported by the National Research Foundation of Korea (NRF) grant funded by the Korea government (MEST) (no. 20110001139).

References

1. K. Nomura, H. Ohta, A. Takagi, T. Kamiya, M. Hirano, and H. Hosono, *Nature*, **432**, 488 (2004).
2. R. L. Hoffman, B. J. Norris, and J. F. Wager, *Appl. Phys. Lett.*, **82**, 733 (2003).
3. J. K. Jeong, J. H. Jeong, H. W. Yang, J.-S. Park, Y.-G. Mo, and H. D. Kim, *Appl. Phys. Lett.*, **91**, 113505 (2007).
4. H. Q. Chiang, J. F. Wager, R. L. Hoffman, J. Jeong, and D. A. Keszler, *Appl. Phys. Lett.*, **86**, 013503 (2005).
5. E. M. C. Fortunato, L. M. N. Pereira, P. M. C. Barquinha, A. M. B. D. Rego, G. Goncalves, A. Vila, J. R. Morante, and R. F. P. Martins, *Appl. Phys. Lett.*, **92**, 222103 (2008).
6. E. M. C. Fortunato, P. M. C. Barquinha, A. C. M. B. G. Pimentel, A. M. F. Gonçalves, An. J. S. Marques, R. F. P. Martins, and L. M. N. Pereira, *Appl. Phys. Lett.*, **85**, 2541 (2004).
7. N. L. Dehuff, E. S. Kettenring, D. Hong, H. Q. Chiang, J. F. Wager, R. L. Hoffman, C. H. Park, and D. A. Keszler, *J. Appl. Phys.*, **97**, 064505 (2005).
8. D. H. Lee, Y. J. Chang, G. S. Herman, and C. H. Chang, *Adv. Mater.*, **19**, 843 (2007).
9. B. S. Ong, C. Li, Y. Li, Y. Wu, and R. Loutfy, *J. Am. Chem. Soc.*, **129**, 2750 (2007).
10. H.-C. Cheng, C.-F. Chen, and C.-Y. Tsay, *Appl. Phys. Lett.*, **90**, 012113 (2007).
11. S.-J. Seo, Y. H. Hwang, and B.-S. Bae, *Electrochem. Solid-State Lett.*, **13**, H357 (2010).
12. P. K. Nayak, T. Busani, E. Elamurugu, P. Barquinha, R. Martins, Y. Hong, and E. Fortunato, *Appl. Phys. Lett.*, **97**, 183504 (2010).
13. S. T. Meyers, J. T. Anderson, C. M. Hung, J. Thompson, J. F. Wager, and D. A. Keszler, *J. Am. Chem. Soc.*, **130**, 17603 (2008).
14. S. Maekawa and T. Ohishi, *J. Non-Cryst. Solids*, **169**, 207 (1994).
15. M. L. Calzada, A. González, R. Poyato, and L. Pardo, *J. Mater. Chem.*, **13**, 1451 (2003).
16. I. Bretos, R. Jiménez, E. Rodriguez-Castellón, J. Garciá-López, and M. L. Calzada, *Chem. Mater.*, **20**, 1443 (2008).
17. N. Tohge, K. Shinmou, and T. Minami, *J. Sol-Gel Sci. Technol.*, **2**, 581 (1994).
18. M. L. Calzada, I. Bretos, R. Jiménez, H. Guillon, and L. Pardo, *Adv. Mater.*, **16**, 1620 (2004).
19. S.-J. Seo, C. G. Choi, Y. H. Hwang, and B.-S. Bae, *J. Phys. D: Appl. Phys.*, **42**, 035106 (2009).
20. D. W. Barnum, *J. Inorg. Nucl. Chem.*, **21**, 221 (1961).
21. S. Hirai, K. Shimakage, and M. Sekiguchi, *J. Am. Ceram. Soc.*, **82**, 2011 (1999).
22. I. Bretos, R. Jiménez, J. Garciá-López, L. Pardo, and M. L. Calzada, *Chem. Mater.*, **20**, 5731 (2008).
23. M. Chen, Z. L. Pei, C. Sun, L. S. Wen, and X. Wang, *J. Cryst. Growth*, **220**, 254 (2000).